Original paper

Ultrastructure of mitochondria and damage to small blood vessels in siblings with the same mutation in the *NOTCH3* and coexisting diseases

Paulina Felczak[1], Agnieszka Cudna[2], Beata Błażejewska-Hyżorek[3], Julia Buczek[3], Iwona Kurkowska-Jastrzębska[3], Tomasz Stępień[1], Albert Acewicz[1], Teresa Wierzba-Bobrowicz[1]

[1]Department of Neuropathology, Institute of Psychiatry and Neurology, Warsaw, Poland
[2]Neuroimmunology Laboratory at the II Department of Neurology, Institute of Psychiatry and Neurology, Warsaw, Poland
[3]II Department of Neurology, Institute of Psychiatry and Neurology, Warsaw, Poland

We performed ultrastructural studies of mitochondria and evaluated the appearance of small blood vessels of three middle-aged siblings affected by the same mutation in the *NOTCH3* gene, causing CADASIL. CADASIL pathognomonic features include granular osmiophilic material (GOM), which we observed. GOMs were located in damaged and thickened basement membranes (BM) of capillaries and arterioles. Our patients were also burdened by type II diabetes (first patient), impaired glucose metabolism (second patient), and hypertension (third patient). The ultrastructure of the capillaries in the first and second patients differed from the third patient. In diabetes/impaired glucose metabolism patients (first and second patients), we observed: pathologies of mitochondria in damaged endothelium and pericytes of capillaries; extremely thickened (BM) with visible remains of vascular cells; well-preserved GOMs anchored in the rebuilt capillary extracellular matrix. We identified degenerated or vestigial small blood vessels of skeletal muscles in the first patient. The capillary damage in the third patient (with hypertension) was milder compared to the diabetes/impaired glucose metabolism patients. We conclude that in patients with a mutation in the *NOTCH3* gene, the co-occurrence of diseases such as type II diabetes/impaired glucose metabolism can cause a multiplication the damages to small blood vessels by modifying/masking the pathogenesis of CADASIL.

Key words: damages of mitochondria, GOM deposits, *NOTCH 3* mutation, diabetes, ultrastructure.

Introduction

Mitochondria are double-membranous organelles containing their own DNA and translation system. They play a central role in cell homeostasis [1, 2]. In healthy vascular systems, mitochondria regulate various processes, in addition to providing ATP to the vascular cells. In diseased human vascular tissues, mitochondria change morphologically and functionally [3]. Mitochondria are also an integral part of a cytoplasmic Notch-activated signaling cascade that regulates cell survival [4]. Mutations in genes encoding Notch receptors or ligands lead to a variety of congenital disorders in humans. Humans express four Notch receptors (Notch1-Notch4) and five different Notch ligands [5]. Mutations in the *NOTCH3*

gene are the cause of **C**erebral **A**utosomal **D**ominant **A**rteriopathy with **S**ubcortical **I**nfarcts and **L**eukoencephalopathy (CADASIL) [6]. The *NOTCH3* maps to the short arm of chromosome 19 (19p13.2-p13.1) and is a large gene containing 33 exons. It encodes the Notch 3 receptor protein, predominantly expressed in adults by vascular smooth muscle cells and pericytes [7]. More than 200 different *NOTCH3* CADASIL-associated mutations have been reported; the majority of them missense substitutions of a single base leading to loss or gain of a cysteine residue within one of the EGFRs of the Notch 3 extracellular domain. Most mutations were found to cluster in exons 3 and 4 and account for approximately 70% diagnosed with a CADASIL mutation, [8] but there are also many reports of mutations in other exons encoding the extracellular portion of the protein [7].

CADASIL is the most common hereditary subcortical vascular dementia. The main clinical features of CADASIL are migrainous headache with aura, recurrent ischemic attacks, cognitive decline, and psychiatric symptoms [9]. CADASIL patients usually display diffuse white-matter changes in deep white matter, with external capsules and anterior pole of temporal lobes in the MRI imaging [10]. While clinical symptoms and mutations vary between patients, the pathognomonic feature in all CADASIL patients is the accumulation of granular osmiophilic material (GOM) in the walls of small arteries on ultrastructural examination [10, 11]. GOM deposits within the tunica media of the damaged vessels is a typical finding in affected patients. GOMs appear as 0.2–2 mm-sized osmiophilic and periodic-acid Schiff-positive granules located around degenerating vascular smooth muscle cells (VSMCs) [12] generally from medium-sized or small arterioles (outer diameter 20-40 μm) [13]. However, in a few cases, GOM has also been detected in veins [13] and capillaries [14]. GOM deposits were first reported in the media of the small cerebrum-penetrating arteries [15]. This material has also been detected in vessels of extracerebral tissues, on arterial smooth muscle cells in the skin, retina, muscle, and peripheral nerves, and represent a golden standard for diagnosis of CADASIL via electron micrographic imaging [11]. Skin biopsies are an important diagnostic tool, [16] with a specificity of 100%, and variable sensitivity from 45% to 100% according to different reports [7, 13].

In patients affected by CADASIL, the accumulation of extracellular matrix (ECM) proteins (including collagens, fibronectin, and vimentin) in the small vessels outside the degenerating VSMCs, causes the thickening of the vessel walls [13]. The thickening of the basement membrane (BM) occurs in normal aging and is a common finding in arteries and capillaries. Basement membrane reduplication is observed in many myopathies and neurogenic atrophies; it is thought to be caused by multiple cycles of capillary degeneration and regeneration. Hypertensive patients frequently have thickened BMs, and one cause of this is increased vascular resistance. Patients with diabetes mellitus, particularly type 2, frequently have aging and hypertensive vascular changes, as well as additional damage caused by their diabetic condition [17].

Our study aimed to compare the ultrastructure of mitochondria and assess the damage to small blood vessels, capillaries, and arterioles in three siblings with the same mutation in the *NOTCH3*. These individuals had comorbidities such as type II diabetes, impaired glucose metabolism, and hypertension.

Case reports

First case

A 47-year-old man with suspected CADASIL was admitted to the Department of Neurology. Brain magnetic resonance imaging (MRI) showed T2- and FLAIR-hyperintense, confluent areas in the periventricular and subcortical white matter of both hemispheres including anterior temporal lobes, and external capsules with multiple, bilateral, periventricular lacunar infarctions (Fig. 1). Medical history indicated that the patient had an ischemic stroke of the left hemisphere eight years earlier, along with right-sided hemiparesis. In the past, the patient has been diagnosed with type II diabetes, a history of acute pancreatitis, and lipid disorders. From 17 years of age, the patient smoked up to 30 cigarettes a day and

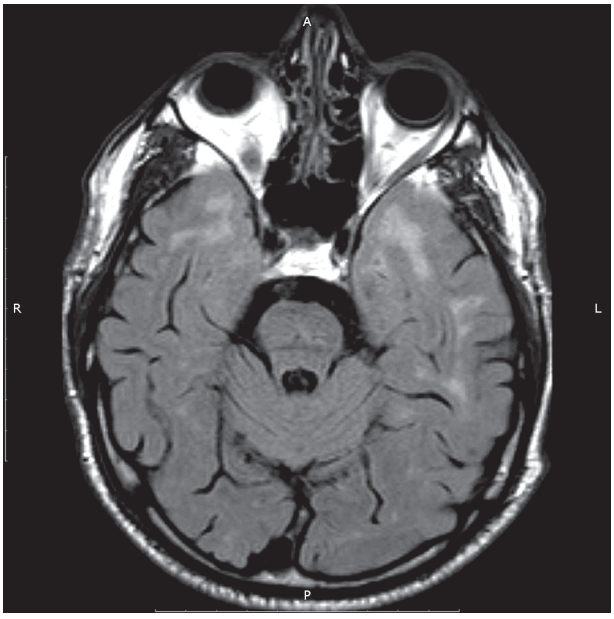

Fig. 1. Patient 1. Brain MRI. Confluent hyperintense areas in the white matter of anterior temporal lobes in FLAIR images

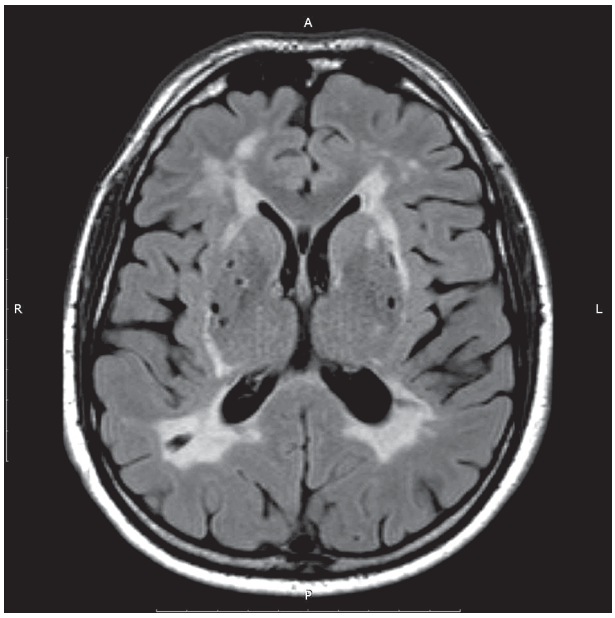

Fig. 2. Patient 2. Brain MRI. Confluent increase signal intensity in the bilateral external capsules with multiple lacunar infarctions in the bilateral basal ganglia in FLAIR images

abused alcohol for about 15 years. In blood tests, he had fasting glucose (glucose 180.0 mg/dl, norm: 70.0-99.0) and elevated levels of total cholesterol, LDL cholesterol, and triglycerides.

Second case

A 50-year-old man, the brother of the first patient, was admitted to the Department of Neurology with progressive paresis of the left limbs. Brain MRI showed confluent increased signal intensity in T2-weighted and FLAIR images in the white matter of both hemispheres, including external capsules and anterior temporal lobes with multiple, bilateral lacunar infarctions (Fig. 2). Medical history indicated that the patient had an ischemic stroke in the form of right-sided hemiparesis with speech disorders fifteen years earlier. After another ischemic stroke one year ago, a new ischemic focus in the left hemisphere of the brain was detected in an MRI of the brain. At a young age, he smoked large quantities of cigarettes. Laboratory tests confirmed impaired glucose metabolism (glucose 110.2 mg/dl, norm: 70.0-99.0) and lipid metabolism disorders.

Third case

A 48-year-old woman, sister of the first and second patients, with severe headaches after an ischemic stroke, was admitted to the Department of Neurology. Brain MRI revealed confluent, bilateral hyperintense areas in the white matter of the frontal, parietal, temporal, and occipital lobes in T2 and FLAIR sequences. The patient also had transient ischemic attacks (TIAs) in the form of transient half-sensory disorders. The patient's medical history demonstrated that she suffered from headaches that have occurred since high school, and for 20 years were very severe, localized in the frontal and occipital areas, with blown eyeballs. In addition, she was diagnosed with depression and was treated for hypertension.

All three patients had blood taken for genetic testing, and skin and skeletal muscle biopsy samples for ultrastructural examinations.

Materials and methods

Material derived from First Polish Brain Bank in Institute Psychiatry and Neurology in Warsaw. The ultrastructural investigations were performed on samples derived from skin and muscle biopsies from biceps three siblings aged 47-50 with clinically and genetically confirmed CADASIL. For electron microscope evaluation, small fragments of tissues were fixed in 2.5% glutaraldehyde solution in cacodylate buffer pH 7.4 and postfixed in 1% osmium tetroxide solution in the same buffer. After dehydration in a graded ethanol alcohol series and propylene oxide, specimens were embedded in Spurr resin. Semithin sections were stained with toluidine blue to choose the appropriate areas. Ultrathin sections were contrasted with uranyl acetate and lead citrate. The sections were examined and photographed with a transmission electron microscope (TEM) JEOL model 140 at the Nencki Institute of Experimental Biology PAS in Warsaw.

Molecular data

Our patients had the same mutation in the *NOTCH3*; this was a heterozygous missense mutation in exon 4; 553T>T/C (nucleotide change) and p. C185R (amino acid change).

Results

Ultrastructure

Small blood vessels from three middle-aged siblings (47-50 years old) were subject to ultrastructural examination. Capillaries and/or arterioles were examined. The vessels were derived from skeletal muscles and/or the dermis.

Ultrastructure of the small blood vessels of the first patient

Capillaries

Most capillaries in the skeletal muscles exhibited pathological features (Figs. 3-6). In some capillaries, distorted endothelial cells (EC) surrounded the creviced lumen of the vessels (Fig. 3). In most of the

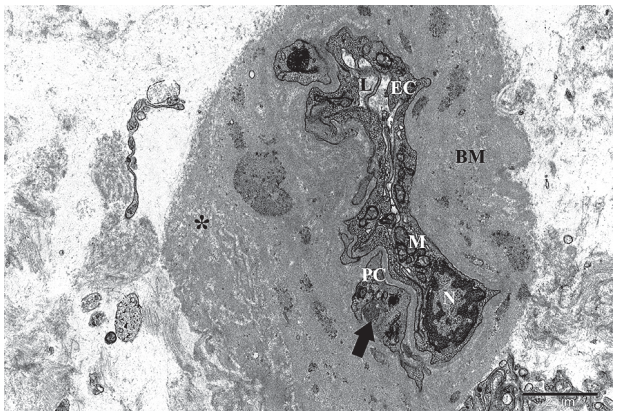

Fig. 3. Patient 1. Capillary with damaged mitochondria (M) in deformed endothelial cells (EC). GOM deposit (arrow) locates near degenerate pericyte (PC) in a thickened heterogeneous basement membrane (BM) with the features of disintegration (asterisk). Nucleus (N), creviced lumen (L). Original magnification 12,000×

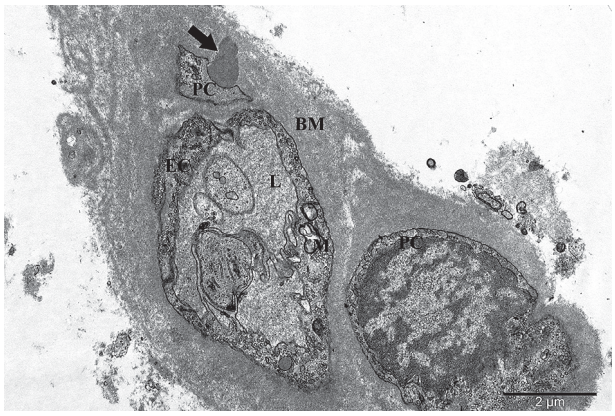

Fig. 4. Patient 1. Capillary with swollen endothelial cells (EC) with damaged mitochondria (M). GOM deposit (arrow) locates near degenerate pericyte (PC) in thickened basement membrane (BM). Lumen (L). Original magnification 15,000×

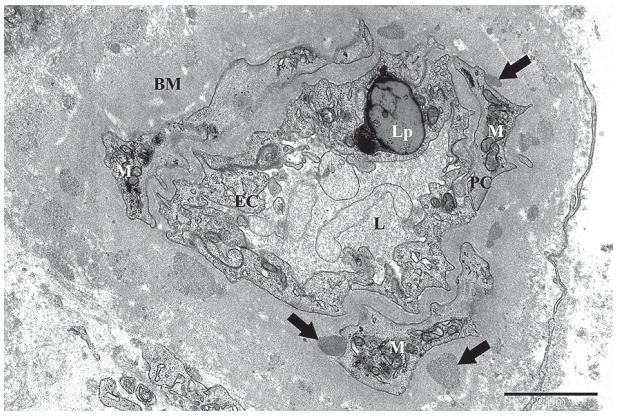

Fig. 5. Patient 1. Capillary with swollen endothelial cells (EC) and clusters of mitochondria (M) in pericytes (PC). GOM deposits (arrow) locate in a thickened heterogeneous basement membrane (BM). Lipofuscin (Lp), lumen (L). Original magnification 15,000×

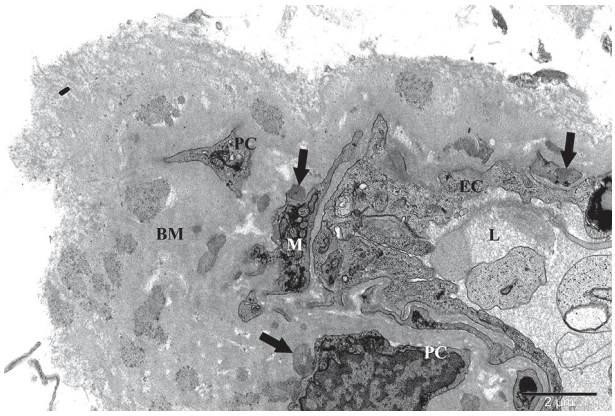

Fig. 6. Patient 1. Fragment of capillary. Extremely thickened heterogeneous basement membrane (BM) with GOM deposits (arrow). Endothelial cell (EC), pericyte (PC), mitochondria (M), lumen (L). Original magnification 12,000×

endothelial cells, finger-like cytoplasmic projections occurred and were visible both from the luminal side and from the abluminal side (Figs. 5, 6). In the cytoplasm of some endothelial cells, rounded nuclei, and densities of heterochromatin under the nuclear envelope were visible (Fig. 3). Numerous pinocytic vesicles (Figs. 4, 5, 6), small vacuoles, few rough endoplasmic reticulum (RER), and lipofuscin deposits were found in the cytoplasm of ECs (Fig. 5). Endothelial mitochondria were fine, oval, or rod-shaped, usually with high electron density with visible cristae (Figs. 3, 5). Mitochondria with cristae defects and a bright matrix were also found (Fig. 4). The number of mitochondria in the narrow endothelial cytoplasm was limited to 1-2 per cell (Fig. 5), while in thicker bands of cytoplasm, up to 3-4 or more mitochondria per EC were found (Fig. 3). In addition to ECs, pericytes (PC) were observed. These cells differed in morphology and density in the walls of the capillaries. Some of them were small (Fig. 3), medium (Fig. 5), large (Fig. 4), or different in size within one capillary (Figs. 4, 6). The shapes of smaller PCs were irregular (Fig. 3), semicircular with processes of different lengths directed towards the endothelium and/or in the opposite direction (Figs. 5, 6). In smaller pericytes, clusters of mitochondria were often visible in the cytoplasm. These oval or elongated organelles contained a dense matrix with poor or residual cristae (Figs. 5, 6). Pinocytic vesicles, short ER (Figs. 5, 6), and osmiophilic glycogen deposits (Figs. 3, 5) were also present in these cells. Large PCs were rounded (Figs. 4, 6) and contained nuclei with dense heterochromatin, surrounded by narrow strands of cytoplasm. In capillaries, the basement membranes (BM) were thick (Figs. 3, 4, 5), and in some vessels extremely thickened (Fig. 6). The ultrastructure of these

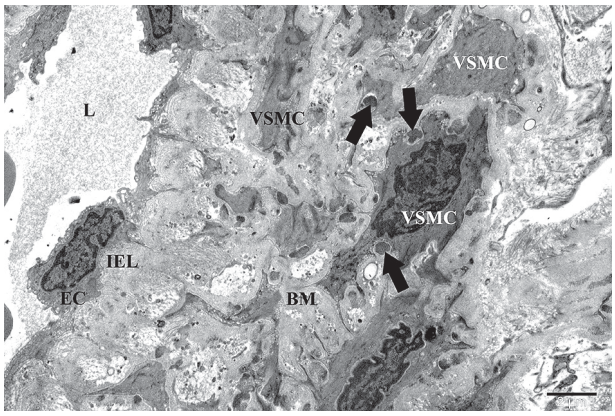

Fig. 7. Patient 1. Arteriole with damaged vascular smooth muscle cells (VSMC). GOM deposits (arrow) locate in cavities the basement membrane (BM) in the tunica media. Endothelial cell (EC), internal elastic lamina (IEL), lumen (L). Original magnification 8,000×

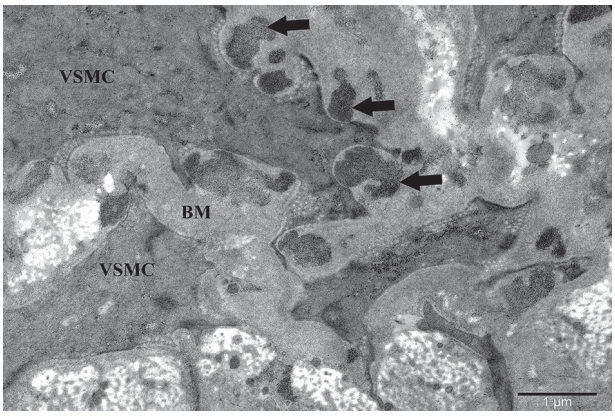

Fig. 8. Patient 1. In arteriole, in the vicinity of myocytes (VSMC), GOM deposits (arrow) visible in the basement membrane (BM). Original magnification 25,000×

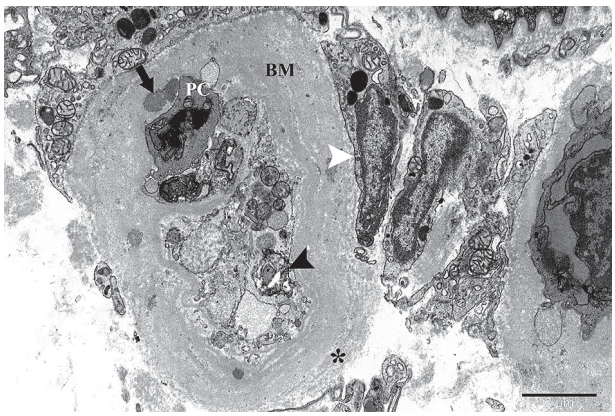

Fig. 9. Patient 1. A degenerated small blood vessel. GOM deposit (arrow) locates near pericyte (PC) in the thickened heterogeneous basement membrane (BM) with the features of disintegration (black asterisk). Remains of damaged vascular cells (black arrowhead) in lumen filled. In the vicinity of the vessel wall, polygonal cells visible (white arrowhead). Original magnification 12,000×

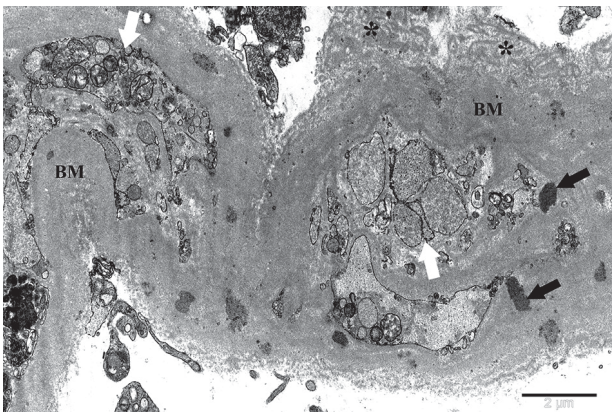

Fig. 10. Patient 1. Extremely thickened and deformed basement membranes (BM) of degenerated small vessels with preserved GOM deposits (black arrow) and with the features of disintegration (black asterisk). Remains of damaged vascular cells (white arrow) in the lumen. Original magnification 12,000×

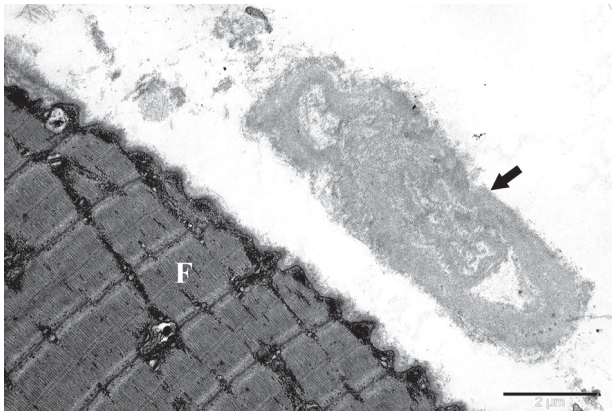

Fig. 11. Patient 1. Residues of wall material from the blood vessel (arrow). Skeletal muscle fiber (F). Original magnification 15,000×

BMs was most often heterogeneous, with features of delamination of wall components and retrograde changes (Fig. 3). Deposits of GOM were observed in BMs of all capillaries studied (Figs. 3-6). These deposits differed in size, shape, and density (Figs. 3-6). In the vessel walls, GOMs were most often found in cavities or indentations of pericyte membranes (Figs. 4, 5) or their vicinity. GOM deposits were often visible in cross-section throughout of the BM (Figs. 3, 5, 6).

Arterioles

Enlarged ECs were visible from the lumen side of the vessel in damaged the skin arterioles (Fig. 7). In the cytoplasm of ECs, large, electron-dense nuclei were observed. Deeper, under the endothelium, a thick internal elastic lamina (IEL) was pres-

ent. The vascular smooth muscle cells (VSMC) were disturbed and were characterized by irregular cell distribution in the vessel wall structure. Myocytes of this layer differed in appearance and size (Figs. 7, 8). Some of them retained fusiform shapes or were irregular, while degenerative features and diminutive structure characterized most of the muscle cells. In the cytoplasm of some myocytes, large nuclei with osmiophilic dense of heterochromatin under the nuclear envelope were visible. In degenerate cells, the arrangement of cytoskeleton elements was often disordered, as was the structure of the organelles. The distances between adjacent damaged muscle cells were increased by structurally changed BM (Fig. 7). The BM surrounding myocytes was significantly thickened and heterogeneous, with bright areas at the losses sites of matrix components that co-formed the vessel wall. Extracellular GOM deposits in the form of aggregation of heterogeneous material were observed in the BM of myocytes. GOMs differed in electron density, size and shape, and were most often irregular or less often semicircular near of myocyte membranes (Figs. 7, 8).

Deformations of small blood vessels

In the small blood vessels of the first patient, various forms of wall deformation and degeneration of vascular cells often occurred (Figs. 9, 10, 11). Degenerated endothelium components were observed in the lumens of damaged vessels. They were osmiophilic vesicles and vacuoles of various sizes filled with heterogeneous material. In the peripheral parts of the damaged vessels, residual non-uniform material was found, the location of which corresponded to degenerated pericytes (Fig. 9). In deformed vessels was extremely thickened BMs showing signs of disintegration of various degrees (Figs. 9, 10). Clusters of osmiophilic material in the thickened walls of damaged vessels were often observed. Conglomerates of this material resembled the appearance and location GOM deposits well preserved in these places (Fig. 10). Polygonal cells of varying sizes were observed in the vicinity of the damaged vessels, and some of them contained large nuclei and dense cytoplasm (Fig. 9). In the vicinity of skeletal muscle fibers, conglomerates that resemble the residual forms of vessels were often observed. They looked like deserted lumens surrounded by disordered fragments of vessel walls (Fig. 11).

Ultrastructure of the small blood vessels of the second patient

Capillaries/arterioles

In the skeletal muscle capillaries endothelial cells showed degenerative features, and differed in thickness and were damaged (Figs. 12, 13, 14). Their

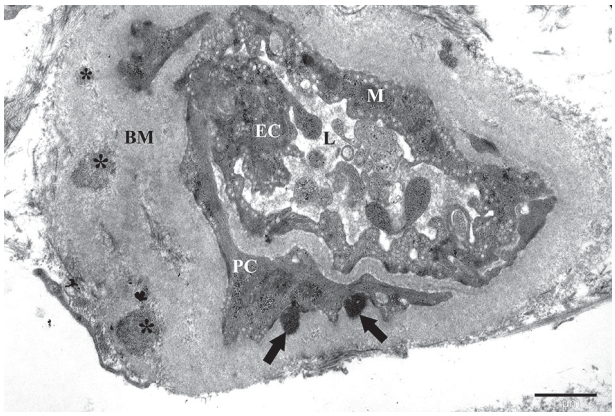

Fig. 12. Patient 2. Capillary with swollen and deformed endothelial cells (EC) and GOM deposits (arrow) locate near semicircular pericyte (PC) in a thickened heterogeneous basement membrane (BM). Clusters of granular material in the BM (black asterisk). Mitochondria (M), lumen (L). Original magnification 20,000×

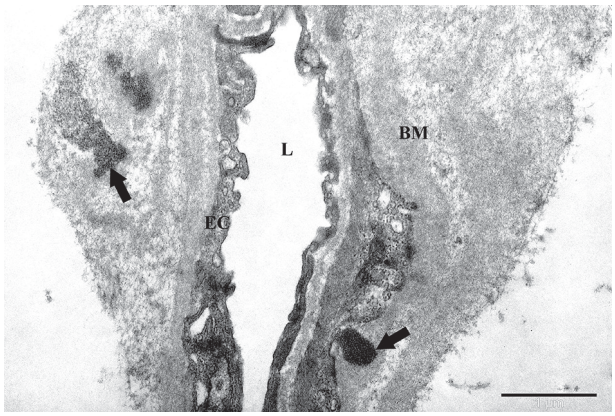

Fig. 13. Patient 2. Capillary with thin endothelial cells (EC) and GOM deposits (arrow) locate in the extremely thickened basement membrane (BM) with damaged structure. Lumen (L). Original magnification 30,000×

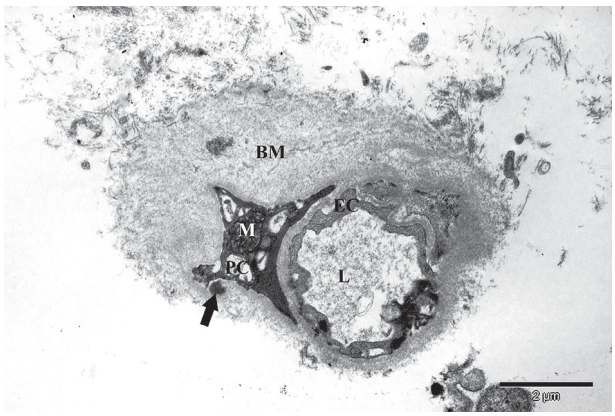

Fig. 14. Patient 2. Capillary with GOM deposit (arrow) locates near degenerate pericyte (PC) in a thickened basement membrane (BM) with a dispersed structure. Endothelial cell (EC), mitochondria (M), lumen (L). Original magnification 15,000×

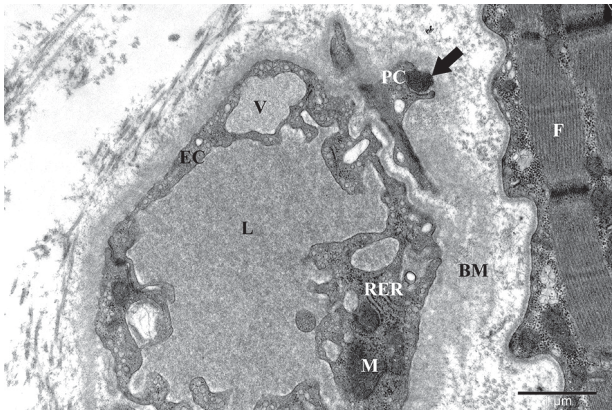

Fig. 15. Patient 3. Capillary with GOM deposit (arrow) locates near pericyte (PC) in the basement membrane (BM) with the features of degeneration. Endothelial cell (EC), vacuole (V), mitochondria (M), rough endoplasmic reticulum (RER), lumen (L), skeletal muscle fiber (F). Original magnification 25,000×

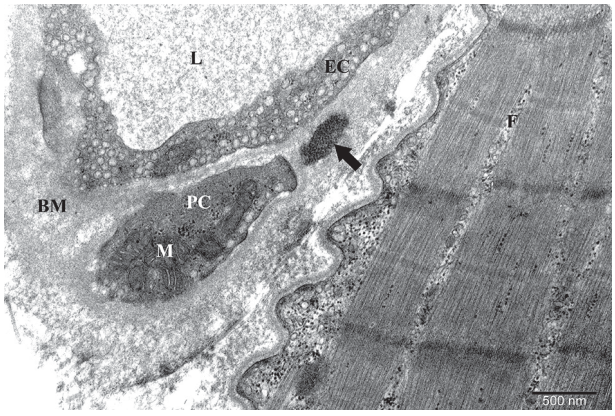

Fig. 16. Patient 3. Fragment of capillary, with numerous pinocytic vesicles in the endothelial cell (EC) and a GOM deposit (arrow) locates in the basement membrane (BM). Pericyte (PC), mitochondria (M), lumen (L), skeletal muscle fiber (F). Original magnification 40,000×

shapes were very irregular and wavy, mainly from the luminal side. In this EC was the blurred integrity of most cellular organelles in a dense cytoplasm. In the swollen endothelial cells, the mitochondria were dark in the background of the cytoplasm, small, oval, and lacking in cristae. Most often, mitochondria were visible in individual endothelial cells (Fig. 12). Pericytes, as well as endothelial cells, showed various stages of degeneration. These pericytes were semicircular (Figs. 12, 13) or star-shaped (Fig. 14). Pericytes differed in size, and the structure of most of the organelles in these cells was distorted (Fig. 13). They contained concentrated cytoplasm or, in extreme cases, strongly osmiophilic with clusters of swollen mitochondria (Fig. 14). Sometimes, dark rounded or irregular GOM deposits were observed near pericytes (Figs. 12, 13, 14). BMs of small vessels were usually significantly thickened with irregular shapes (Figs. 12, 13, 14), homogeneous (Fig. 12), or heterogeneous with features of degradation (Figs. 13, 14). Clusters of granular material of varying density were observed in the peripheral parts of the vessel walls, which resembled the GOM deposits preserved there (Fig. 12). The number of GOMs observed on the cross-sections varied; there were usually several deposits in one capillary (Figs. 12, 13, 14).

The alterations in arterioles of the first and second patients were comparable. The structure was similar in the degree of damage to the myocytes in the tunica media, and the amount and morphology of GOM deposits in the thickened BMs.

Ultrastructure of the small blood vessels of the third patient

Capillaries

Most capillaries showed mild lesions compared to the patient's siblings (Figs. 15, 16). Endothelial cells were deformed and swollen to varying degrees. Different size vacuoles filled with granular material were observed in damaged ECs. Numerous pinocytic vesicles and short RER were detected in dense cytoplasm (Figs. 15, 16). Mitochondria were dark, rounded or elongated with slightly visible cristae. Few mitochondria were found in endothelial cells. Pericytes were small with cytoplasmic projections (Fig. 15) or larger oval (Fig. 16). Mitochondria were the most prominent in the dense PCs cytoplasm, which were often found in clusters. Basement membranes were slightly thickened, heterogeneous, and irregular shapes. Small, dark, single GOM deposits were found in the vessel walls, in the vicinity of pericytes (Figs. 15, 16).

Arterioles

In arterioles deformed and contracted muscle cells were more frequently observed (Fig. 17). In dense cytoplasm, large, rounded nuclei with osmiophilic heterochromatin under the nuclear envelope were detected in some VSMCs. Mitochondria were most commonly found in clusters in smooth muscle cells and were oval or elongated with few cristae (Figs. 17, 18). Dense bodies characteristic of these cells in contact with the membranes of myocytes were observed. The basement membranes surrounding smooth muscle cells were thickened and damaged, with loss of the matrix components. Extracellularly, in the vicinity of myocytes, there were very many GOM deposits (Fig. 18). GOM were densely distributed in the BMs. GOMs differed in size, shape, and density (Figs. 17, 18). The BMs were enlarged and damaged, with defects in structural components (Fig. 17). Extracellularly, in the vicinity of myocytes, there were many deposits of GOM were densely distributed in the basement membranes. GOMs differed in size, shape, and electron density (Figs. 17, 18).

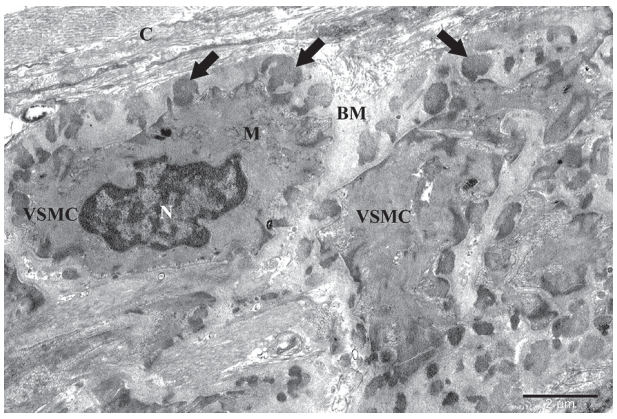

Fig. 17. Patient 3. Arteriole with numerous GOM deposits (arrow) locate in the damaged basement membrane (BM) with visible bright regions with degenerative features, near myocytes (VSMC). Nucleus (N), mitochondria (M), collagen (C). Original magnification 12,000×

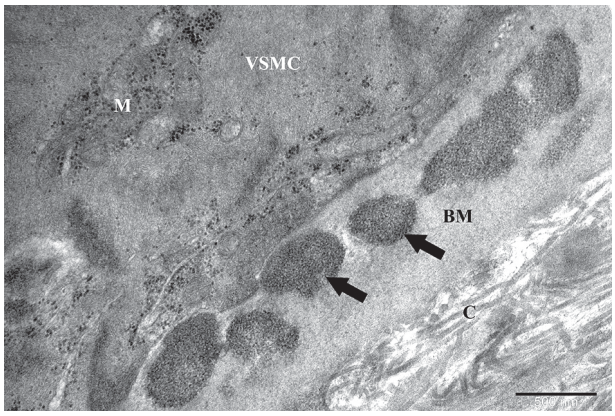

Fig. 18. Patient 3. GOM deposits (arrow) locate in the basement membrane (BM) near myocyte (VSMC). Mitochondria (M), collagen (C). Original magnification 50,000×

Discussion

The Notch signaling pathway is an evolutionary cascade that regulates the development and homeostasis of various tissues, including the vascular system. Aberrant Notch signaling is the cause of many diseases, including CADASIL [18, 19]. Cerebral autosomal dominant arteriopathy with subcortical infarcts and leukoencephalopathy (CADASIL) is hereditary disease causing angiopathy of small blood vessels, and usually affects middle-aged adults [12, 20].

We investigated the case of three middle-aged siblings in which the same mutation 553T>T/C, p.C185R in exon 4 of the *NOTCH 3* was detected. Mutations in this exon are the most common cause of CADASIL. Parallel to genetic testing, the clinical diagnosis of siblings was also carried out. Our patients had prominent signal abnormalities in the brain magnetic resonance imaging (MRI), confirming CADASIL.

Our research focused on the analysis of CADASIL pathology at the ultrastructural level in three siblings. In addition to the recognized CADASIL, the patients studied had coexisting diseases: type II diabetes in the first patient, impaired glucose metabolism in the second patient, and hypertension in the third patient.

We compared the ultrastructure of the capillaries and arterioles of three CADASIL patients. The capillaries in the first and second patients were much more damaged than in the third patient. Pathological changes in siblings' arterioles were milder than in capillaries, and comparable in the three cases examined. Damaged and deformed endothelial cells (EC), pericytes (PC), and vascular smooth muscle cells (VSMC) were observed in the vessels. As well as CADASIL, patients also presented with other diseases such as type II diabetes, impaired glucose metabolism, or hypertension that may damage small vessel cells. The observed EC, PC, and VSMC pathologies should not be treated as characteristic only for CADASIL. These disorders are probably due to the combined effect of these diseases on the ultrastructure of vascular cells.

The dysregulation of the vascular system underlies multiple pathophysiologic processes [21]. For example, endothelium dysfunction is associated with atherosclerosis, hypertension, and diabetes [22]. Pericytes damage has been indicated in hypertension, diabetic retinopathy, Alzheimer's disease, and CNS tumor formation [23]. The abnormal proliferation and migration of VSMCs contribute to hypertension and atherosclerosis [24].

In our study, mitochondria in ECs and PCs were characterized by a dense matrix with few cristae or were bright and swollen. These organelles were observed in singlets or small clusters of 4-5 structures. In degenerated and diminutive VSMCs, mitochondria were difficult to distinguish in the concentrated cytoplasm. In studies of VSMCs in CADASIL patients, carriers of the R133C mutation possessed an increased number of abnormal mitochondria. Measurements of mitochondrial membrane potential showed a lower percentage of functional mitochondria in VSMCs and reduced superoxide dismutase 1 expression. The authors suggested that proliferation and mitochondrial dysfunction in VSMCs may affect vascular cell function in CADASIL pathology [25]. In another study, the activity of respiratory enzyme complexes in muscle biopsies of patients affected by CADASIL was assessed, and a significant decrease in NADH dehydrogenase and cytochrome c oxidase was found, indicating an impairment of the oxidative phosphorylation chain [26].

The pathologies of mitochondria in damaged small vessel cells in our patients, should not be considered as specific for CADASIL, due to the overlapping effects of coexisted diseases. Ultrastructural assessment

of the number of abnormal mitochondria in individual cells of the vascular walls in CADASIL was also problematic. In general, lower mitochondria densities were observed in myocytes of the tunica media of small vessels compared to skeletal muscle fibers. However, our observations also showed that higher densities of damaged mitochondria were found in some disturbed endothelial and pericyte cells in capillaries.

According to the literature, ECs and VSMCs of microvessels exhibit relatively low energy requirements. Glycolysis in these cells under physiological conditions meets such requirements. Mitochondrial ATP production can be reversibly activated without harming these cells. In addition to glycolysis, inhibition of mitochondrial biogenesis and mitophagy, contribute to reducing the number of mitochondria, and consequently to a reduction in oxygen consumption. For comparison, mitochondria in the endothelium account for only 5% of cell volume, while in hepatocytes, they account for up to 28% [27].

We suppose that in ECs and PCs in capillaries, increased amounts of damaged mitochondria may be associated with the mobilization of mitochondrial ATP resources instead of glycolytic resources. As a result, there may be a higher energy demand in vascular cells in CADASIL compared to physiological conditions.

It is known that pathological hallmark of CADASIL is the deposition of GOM in close relation to VSMCs [16]. Our ultrastructural observations showed that deposits of GOM were found in the walls of the small blood vessels of the skeletal muscles and skin of the siblings. GOM deposits were located in the basement membranes (BM) of capillaries and arterioles and differed in structure, distribution, and abundance in BMs.

The molecular composition of GOM is still under investigation. It has been revealed the extracellular domain of Notch 3 (N3ECD) and other matrix proteins involved in blood vessel maintenance, such as tissue inhibitor of metalloproteinases 3, vitronectin, and latent TGF-β binding protein 1, as well as amyloid P, annexin 2, and periostin. Due to its role in the stabilization of amyloid plaques in Alzheimer's disease, amyloid P may play an analogous role in the stabilization of GOM in CADASIL [12].

We observed differences in the distribution of GOM deposits in our CADASIL patients in small blood vessels. GOMs were very numerous and observed in comparable numbers in BM tunica media of arterioles in three siblings. In turn, GOM in capillaries was less frequently observed and was found primarily in the first and second patients. In the third patient, only single GOM deposits in BM of capillary were visible.

The processes leading to GOMs formation are far from understanding. One of several hypotheses assumes that GOM can be assembled within the ER, where mutant Notch 3 aggregates are retained and released in the extracellular space after VSMC apoptosis [12, 28]. In CADASIL, degeneration and loss of VSMCs were observed over the entire length of the affected vessels. Myocytes preserved in the tunica media are usually unevenly shaped or shrunken [16, 29].

Our research has shown that although GOMs were very numerous near myocytes in the three siblings' arterioles, no extremely damaged myocytes were observed, and no apoptosis was found. Perhaps myocytes saved were associated with triggering mechanisms that came from outside of defective Notch signaling caused by a mutation in the *NOTCH 3*. It seems that the existence of such mechanisms could, in some cases, have a protective effect on myocytes in CADASIL.

It is known that mutations in components of the Notch family constrained the pathway's essential functions. The discovery of diseases related to defective Notch signaling began with the analysis of mutations in chromosome 19 of the *NOTCH3* responsible for CADASIL [5, 6]. On the other hand, anti-apoptotic functions of Notch are linked by interactions with molecules such as kinase Akt and nuclear factor κB (NF-κB), constituting nodes across multiple signaling pathways, suggesting that Notch may function as a key molecular sensor regulating cell survival [4].

We compared the damage to the BMs of capillaries and arterioles of our patients. The ultrastructure of the BM of capillaries was problematic. The most damaged, occupied by GOM deposits and often extremely thickened, were the BMs of capillaries of the first and second patients. Only in the third patient, the damage and BM thickness did not deviate significantly from the norm.

The BM is composed of various extracellular matrix (ECM) proteins, such as laminin, collagen IV, perlecan, nidogens, and agrin, which to produced by endothelial cells [17]. For example, type IV collagen and laminin individually self-assemble into superstructures, and both networks are crucial for BM stability. In turn, nidogen and perlecan influence the structural integrity of BM [30]. The walls of the affected blood vessels become thickened and fibrotic in CADASIL due to the deposition of various types of collagens, fibronectin, laminin, and vimentin [11, 13].

We assumed that damage and the extreme thickening BM in the capillaries observed in our patients resulted not only from changes in the chemical composition of ECM proteins in CADASIL pathology but could also be due to the influence of comorbidities

such as type II diabetes in the first patient and impaired glucose metabolism in the second patient. There is a correlation between diabetes mellitus and capillary BM thickening in the skeletal muscle. This structural rearrangement of the capillaries is influenced by hyperglycemia [31]. Different molecular mechanisms underlie BM thickening in diabetes mellitus. Absorption and intracellular glucose oxidation are increased in ECs of people with diabetes. The production of reactive oxygen species (ROS) is also increased, which affects redox-sensitive transcription factors that regulate the gene expression levels of proteins responsible for BM turnover. ROS may also affect the intracellular accumulation of various metabolites, such as glyceraldehyde 3-phosphate, for example. Under these conditions, glycation, the most important process for thickening BM can be activated. Glycation is the non-catalytic addition of fructose, galactose, and to a minor extent, glucose moieties to proteins [31].

Our research showed that well-preserved GOM deposits were observed in damaged, heterogeneous, stratified, extremely thickened BMs of capillaries. It has been shown that GOM deposits are not static, but change in terms of size, morphology, and number during disease course in CADASIL transgenic mice. It was found a progression from initially small round GOMs, to large amorphous deposits seen in the last stages of the disease [12].

It is also known that in diabetics, the degree of cross-linkage in type IV collagen is augmented by glycation, which renders it more resistant to degradation and turnover [31]. In type II diabetes, impaired glucose metabolism, enhanced production of matrix proteins by transforming growth factor-A, and inadequate protein synthesis, alter the thickness and composition of the BM. Reduplication of the BM is also frequently demonstrated. These combined vascular changes are referred to as the microangiopathy of diabetes [17].

In CADASIL patients, leptomeningeal arteries showed large type IV collagen deposits in the tunica media and tunica intima. These types of fibrotic thickening cause restricted blood flow and increase susceptibility to strokes [11]. The type IV collagen is a relatively inelastic molecule, so a thickened BM might be stiffer than a thinner one. This stricture in microvascular elasticity could indirectly affect the dysfunction EC of capillaries [31]. Damage of the BM from injury or pathogenesis is followed by BM remodeling. This consists of *de novo* deposition of BM proteins, self-assembly, and BM network formation. During this process, cell behavior is influenced by altered BM composition as well as exposed cryptic binding sites [30].

We suspect that the stability of GOM deposits observed in extremely thickened BMs of capillaries and their low susceptibility to disintegration could be because proteins forming the BM, such as laminins, fibronectins, and especially type IV collagen were conducive to anchoring and retaining of GOMs in the wall of the damaged vessel. We posit that this is as a result of structural changes, rearrangement, and stiffening of protein chains. Changes in the composition and structure of the BM may have hindered or prevented the natural process of reconstruction or disintegration GOM deposits, which is observed in CADASIL. In addition, the impact of diabetic microangiopathy on the ultrastructural picture of BM damage should be considered.

In our third patient affected by CADASIL, damage to the BMs of the capillaries was the mildest. This patient did not suffer from diabetes but suffered from hypertension. In her arterioles, in tunica media, damaged and thickened BM was observed, but we did not detect any extreme damage.

In patients who had been diagnosed with arterial hypertension, a slight thickening of the capillary BM in skeletal muscle was observed. Only nonsignificant differences in the capillary ultrastructure between hypertensive patients and controls have been observed, suggesting that arterial hypertension is not accompanied by capillary BM accumulation in skeletal muscle [31].

Our observations showed that the capillary walls, particularly the first patient and to a lesser extent the second patient, were multiplied, with visible irregular densities probably of endothelial and pericyte remains. The BM structure was heterogeneous, fibrous-granular, with dense inclusions corresponding to the appearance and location of GOM deposits. In the lumen of the vessels, different sized vacuolar vesicles with osmiophilic material were found. Additionally, numerous small blood vessels of the first patient were extremely damaged, and the walls of the vessels were very thickened and deformed. In the vicinity of degenerated vessels, various-shaped and size cells were present. Often, only clusters of material from wall fragments were visible, probably as remains of damaged vessels.

In diabetics the BM around capillaries is organized into multiple concentric lamellae, between which cellular debris is usually encountered. These are incompletely phagocytized fragments of apoptotic EC or PC. A thickened BM of the capillary in diabetes hinders the transcytotic migration of leukocytes and macrophages through the vessel wall to sites of inflammation. Capillary BM thickening can be caused by repeated cycles of EC and/or PC degeneration and regeneration, which would promote the attraction of phagocytic cells [31]. In our ultrastructural studies, the search for the causes of the death of small vessels was problematic due to the overlapping effects of CADASIL pathology and diabetes.

Research showing a protective function of Notch3 against apoptosis suggested that this form of cell death may have a dominant role in the pathogenesis of CADASIL. Notch3 signaling regulates the expression of anti-apoptotic genes, which modulate the Fas signaling pathway by inhibiting transcription of proapoptotic genes and enhancing expression of anti-apoptotic mediators like c-FLIP, Bcl-2, and c-IAP-1 [26].

Mitochondria constitute an integral part of a Notch-activated signaling cascade that regulates cell survival. Bcl-2 family proteins determine mitochondrial involvement in death cascades [4]. Mitochondria also play an important role in the pathogenesis of small vessels in diabetics.

Exposure to high levels of glucose leads to biochemical, structural, and functional changes EC and VSMC of mature vessels. The biochemical changes include, among others, increased apoptosis induced by oxidative stress, mitochondrial dysfunction, and changes in the metabolism of fatty acid [32]. The involvement of apoptosis in small vessel cell death in both CADASIL and diabetes appears to be significant. However, this process is not only limited to the cell death of small vessels but applies to, for example, apoptosis in cerebral atrophy in CADASIL.

Neuronal apoptosis has been described in the cerebral cortex of individuals with CADASIL. Apoptosis occurred in layers 3 and 5 of the cerebral cortex, and the number of apoptotic neurons in these layers was associated with the extent of white matter lesions and the intensity of axonal damage in the subcortical white matter [33]. In turn, in other studies, using activated caspase 3 immunostaining and in situ end labeling (ISEL), have been identified apoptotic neurons, astrocytes, oligodendrocytes, and microglial and vascular cells in four unrelated cases of CADASIL with different mutations of the *NOTCH3* [34].

Apoptosis, in response to inappropriate cell/ECM interactions, is termed anoikis [35]. When cells lose their regular cell-matrix interactions, the cell cycle arrests, and a specific form of caspase-mediated programmed cell death, anoikis, is initiated [36]. The potential involvement of anoikis in VSMC degeneration and loss in CADASIL has been researched. A study on arterial vessels revealed changes in compounds of vascular ECM. The immune expression of fibronectin in the vascular media was heterogeneous, and sometimes lacking. A lack of fibronectin can cause a break of bounds between VSMC and ECM within focal adhesions and promote cell death *via* an anoikis pathway [37].

The complexity of the process of dying small vessels indicates the activity of various biochemical pathways that lead to the death of selected cell populations in microangiopathy. When analyzing the aging process and death of small vessels, one should consider not only the importance of apoptosis or anoikis but also the so-called premature aging caused by various factors, which occurs regardless of telomeric shortening. In patients affected with CADASIL and coexisting diseases, it is difficult to exclude the importance of this process in the pathogenesis of these disorders.

In summary, the local increase in the number of damaged mitochondria in the capillary endothelium suggests that the mitochondrial source of ATP may be triggered due to the high energy demand of these cells under the conditions of the coexistence of CADASIL and type II diabetes/impaired glucose metabolism. Extreme damage to the basement membranes of the capillaries in diabetes can mask or modify the pathogenesis of CADASIL and overlapping effects of these diseases is observed in the phenotypes of small blood vessels. The co-occurrence of CADASIL and hypertension results in milder capillary damage compared to the coexistence of CADASIL and diabetes. The stability and resistance of GOM deposits to disintegration in the conditions of coexistence of CADASIL and type II diabetes/impaired glucose metabolism may be associated with extreme thickened capillary BMs and remodeling of structural membrane components, such as collagen. Death and loss of endothelium and pericytes, as well as degeneration and destruction of small vessels as a result of progressive wall thickness, may occur in the mechanism of apoptosis.

Acknowledgements

This work is supported by the „Digital Brain – digital collection of Institute Psychiatry and Neurology" (Project No.POPC.02.03.01-00.0042/18). The authors are very grateful to the First Polish Brain Bank in Institute Psychiatry and Neurology, Warsaw Poland.

Authors declare no conflict of interests.

References

1. Wallace DC. Mitochondrial diseases in man and mouse. Science 1999; 283: 1482-1488.
2. Khan NA, Govindaraj P, Meena AK, et al. Mitochondrial disorders: challenges in diagnosis and treatment. Indian J Med Res 2015; 141: 13-26.
3. Tang X, Luo Y-X, Chen H-Z, et al. Mitochondria, endothelial cell function, and vascular diseases. Front Physiol 2014; 5: 1-17.
4. Perumalsamy LR, Nagala M, Sarin A. Notch-activated signaling cascade interacts with mitochondrial remodeling proteins to regulate cell survival. Proc Natl Acad Sci 2010; 107: 6882-6887.
5. Masek J, Andersson ER. The developmental biology of genetic Notch disorders. Development 2017; 144: 1743-1763.
6. Joutel A, Corpechot C, Ducros A, et al. Notch3 mutations in CADASIL, a hereditary adult-onset condition causing stroke and dementia. Nature 1996; 383: 707-710.

7. Di Donato I, Bianchi S, De Stefano N, et al. Cerebral Autosomal Dominant Arteriopathy with Subcortical Infarcts and Leukoencephalopathy (CADASIL) as a model of small vessel disease: update on clinical, diagnostic, and management aspects. BMC Med 2017; 15: 1-12.
8. Joutel A, Vahedi K, Corpechot C, et al. Strong clustering and stereotyped nature of Notch3 mutations in CADASIL patients. Lancet 1997a; 350: 1511-1515.
9. Tikka S, Mykkanen K, Ruchoux MM, et al. Congruence between NOTCH3 mutations and GOM in 131 CADASIL patients. Brain 2009; 132: 933-939.
10. He D, Chen D, Li X, et al. The comparisons of phenotype and genotype between CADASIL and CADASILlike patients and population-specific evaluation of CADASIL scale in China. J Headache Pain 2016; 17: 1-9.
11. Panahi M. CADASIL: a pure model for studying cerebral small vessel disease. Doctoral dissertation. Published by Karolinska Institutet, Stockholm 2019; 1-59.
12. Locatelli M, Padovani A, Pezzini A. Pathophysiological mechanisms and potential therapeutic targets in cerebral autosomal dominant arteriopathy with subcortical infarcts and leukoencephalopathy (CADASIL). Front Pharmacol 2020; 11: 1-13.
13. Tikka S, Mykkanen K, Junna M, et al. Diagnosing vascular dementia by skin biopsy – uniqueness of CADASIL. In: Khopkar U. Skin Biopsy - Perspectives Vol 9, Publisher In Tech 2011; 183-194.
14. Lewandowska E, Szpak GM, Wierzba-Bobrowicz T, et al. Capillary vessel wall in CADASIL angiopathy. Folia Neuropathol 2010; 48: 104-115.
15. Baudrimont M, Dubas F, Joutel A, et al. Autosomal dominant leukoencephalopathy and subcortical ischemic stroke. A clinicopathological study. Stroke 1993; 24: 122-125.
16. Ruchoux MM, Guerouaou D, Vandenhaute B, et al. Systemic vascular smooth muscle cell impairment in cerebral autosomal dominant arteriopathy with subcortical infarcts and leukoencephalopathy. Acta Neuropathol 1995; 89: 500-512.
17. Buckley AF, Bossen EH. Skeletal muscle microvasculature in the diagnosis of neuromuscular disease. J Neuropathol Exp Neurol 2013; 72: 906-918.
18. Nowell C, Radtke F. Cutaneous notch signaling in health and disease. Cold Spring Harb Perspect Med 2013; 3: 1-15.
19. Fouillade Ch, Monet-Lepreˆtre M, Baron-Menguy C, et al. Notch signalling in smooth muscle cells during development and disease. Cardiovasc Res 2012; 95: 138-146.
20. Opherk C, Peters N, Herzog J, et al. Long-term prognosis and causes of death in CADASIL: a retrospective study in 411 patients. Brain 2004; 127: 2533-2539.
21. Kutcher ME, Herman IM. The pericyte: cellular regulator of microvascular blood flow. Microvasc Res 2009; 77: 235-246.
22. Sena CM, Pereira AM, Seiça R. Endothelial dysfunction – A major mediator of diabetic vascular disease. Biochim Biophys Acta 2013; 1832: 2216-2231.
23. Allt G, Lawrenson JG. Pericytes: cell biology and pathology. Cells Tissues Organs 2001; 169: 1–11.
24. Qiu J, Zheng Y, Hu J. Biomechanical regulation of vascular smooth muscle cell functions: from in vitro to in vivo understanding. J R Soc Interface 2014; 11: 1-13.
25. Viitanen M, Sundstrom E, Baumann M, et al. Experimental studies of mitochondrial function in CADASIL vascular smooth muscle cells. Exp Cell Res 2013; 319: 134-143.
26. Formichi P, Radi E, Battisti C. Apoptosis in CADASIL: an in vitro study of lymphocytes and fibroblasts from a cohort of Italian patients. J Cell Physiol 2009; 219: 494-502.
27. Dromparis P, Michelakis ED. Mitochondria in vascular health and disease. Annu Rev Physiol 2013; 75: 95-126.
28. Takahashi K, Adachi K, Yoshizaki K, et al. Mutations in NOTCH3 cause the formation and retention of aggregates in the endoplasmic reticulum, leading to impaired cell proliferation. Hum Mol Genet 2010; 19: 79-89.
29. Dziewulska D, Nycz E, Rajczewska-Oleszkiewicz C, et al. Nuclear abnormalities in vascular myocytes in cerebral autosomal-dominant arteriopathy with cubcortical infarcts and leukoencephalopahty (CADASIL). Neuropathol 2018; 38: 601-608.
30. LeBleu VS, MacDonald B, Kalluri R. Structure and function of basement membranes. Exp Biol Med 2007; 232: 1121-1129.
31. Baum O, Bigler M. Pericapillary basement membranę thickening in human skeletal muscle. Am J Physiol Heart Circ Physiol 2016; 311: H654-H666.
32. Madonna R, Balistreri CR, Geng Y-J, et al. Diabetic microangiopathy: pathogenetic insights and novel therapeutic approaches. Vasc Pharmacol 2017; 90: 1-7.
33. Viswanathan A, Gray F, Bousser M-G, et al. Cortical neuronal apoptosis in CADASIL. Stroke 2006; 37: 2690-2695.
34. Gray F, Polivka M, Viswanathan A, et al. Apoptosis in cerebral autosomal dominant arteriopathy with subcortical infarcts and leukoencephalopathy. J Neuropathol Exp Neurol 2007; 66: 597-607.
35. Gilmore AP. Anoikis. Cell Death Differ 2005; 12: 1473-1477.
36. Guadamillas MC, Cerezo A, Del Pozo MA. Overcoming anoikis – pathways to anchorage independent growth in cancer. J Cell Sci 2011; 124: 3189-3197.
37. Dziewulska D, Nycz E, Rajczewska-Oleszkiewicz C. Changes in the vascular extracellular matrix as a potential cause of myocytes loss via anoikis in Cerebral Autosomal Dominat Arteriopathy with Subcortical Infarcts and Leukoencephalopathy. J Clin Exp Pathol 2017; 7: 1-5.

Address for correspondence

Paulina Felczak
Department of Neuropathology
Institute of Psychiatry and Neurology
Sobieskiego 9
02-957 Warsaw, Poland
tel.: + 48 22 45 82 646
e-mail: pfelczak@ipin.edu.pl